

Axisymmetric toroidal modes of magnetized neutron stars

Umin Lee^{1*}

¹*Astronomical Institute, Tohoku University, Sendai, Miyagi 980-8578, Japan*

Typeset 2 February 2008; Received / Accepted

ABSTRACT

We calculate axisymmetric toroidal modes of magnetized neutron stars with a solid crust. We assume the interior of the star is threaded by a poloidal magnetic field that is continuous at the surface with the outside dipole field whose strength B_p at the magnetic pole is $B_p \sim 10^{16}$ G. Since separation of variables is not possible for oscillations of magnetized stars, we employ finite series expansions of the perturbations using spherical harmonic functions to represent the angular dependence of the oscillation modes. For $B_p \sim 10^{16}$ G, we find distinct mode sequences, in each of which the oscillation frequency of the toroidal mode slowly increases as the number of radial nodes of the eigenfunction increases. The frequency spectrum of the toroidal modes for $B_p \sim 10^{16}$ G is largely different from that of the crustal toroidal modes of the non-magnetized model, although the frequency ranges are overlapped each other. This suggests that an interpretation of the observed QPOs based on the magnetic toroidal modes may be possible if the field strength of the star is as strong as $B_p \sim 10^{16}$ G.

Key words: stars: neutron – stars: oscillations – stars : magnetic fields

1 INTRODUCTION

Recent discovery of quasi-periodic oscillations (QPOs) of magnetar candidates is one of the observational manifestations of global oscillations of neutron stars. Israel et al (2005) detected QPOs of frequencies ~ 18 , ~ 30 and ~ 92.5 Hz in the tail of the SGR 1806-20 hyperflare observed December 2004, and suggested that the 30 Hz and 92.5 Hz QPOs could be caused by seismic vibrations of the neutron star crust (see, e.g., Duncan 1998). Later on, in the hyperflare of SGR 1900+14 detected August 1998, Strohmayer & Watts (2005) found QPOs of frequencies 28, 53.5, 84, and 155 Hz, and claimed that the QPOs could be identified with the low l fundamental toroidal torsional modes of the solid crust of the neutron star. These recent discoveries of QPOs in the giant flares of Soft Gamma-Ray Repeaters SGR 1806-20 (Israel et al 2005, Watts & Strohmayer 2006, Strohmayer & Watts 2006) and SGR 1900+14 (Strohmayer & Watts 2005) have made promising asteroseismology for magnetars, neutron stars with an extremely strong magnetic field (see, e.g., Woods & Thompson 2006 for a review of SGRs).

It is currently common to identify these QPOs with seismic vibrations caused by crustal toroidal modes of the neutron stars, since the frequency range of the modes overlap that of the observed QPOs and from the energetics point of view the crustal toroidal modes would be most easily excited to observable amplitudes by spending a least amount of available energies, for example, those released in magnetic field restructuring (e.g., Duncan 1998). Although the interpretation based on crustal torsional modes looks promising, we need detailed theoretical analyses of oscillations of magnetized neutron stars so that we could get information of physical conditions of the stars through the confrontation between theoretical modelings and observations. This is particularly true for high frequency QPOs (e.g., 625 Hz QPO, Watts & Strohmayer 2006; 1835 Hz QPO and less significant QPOs at 720 and 2384 Hz in SGR 1806-20, Strohmayer & Watts 2006), since there exist classes of modes other than the crustal toroidal modes that can generate the frequencies observed.

The presence of a magnetic field makes it possible for toroidal modes to exist in a fluid star even without rotation as does the presence of the shear modulus in the solid crust. In this paper we are interested in axisymmetric toroidal modes since axisymmetric toroidal and spheroidal modes are decoupled for a poloidal field when the star is non-rotating. For non-axisymmetric modes, the toroidal and spheroidal components are coupled even without rotation and hence the modal analyses of magnetized stars would be much more complicated.

* E-mail: lee@astr.tohoku.ac.jp

Theoretical calculations of toroidal modes of strongly magnetized neutron stars have been carried out by several authors, including Piro (2005), Glampedakis et al (2006), Sotani et al (2006, 2007), and Lee (2007). The analyses by Piro (2005), Glampedakis et al (2006), and Lee (2007) assume Newtonian gravity, while those by Sotani et al (2006, 2007) use general relativistic formulation. Although the studies by Piro (2006) and Lee (2007) ignore the effects of magnetic fields in the fluid core, those by Glampedakis et al (2006) and Sotani et al (2006, 2007) consider magnetic waves propagating in the fluid core, assuming the core is threaded by a magnetic field of substantial strength. Besides the differences mentioned above, most of the authors except Lee (2007) represent the angular dependence of the oscillations by a single spherical harmonic function $Y_l^m(\theta, \phi)$. Since the shear modulus in the crust dominates the magnetic pressure in most parts of the crustal regions for a dipole field of strength $B_p \lesssim 10^{15}$ G, this treatment may be justified so long as the crustal toroidal modes are well decoupled from the fluid core. But, if the torsional waves in the crust are strongly coupled with magnetic waves in the core, the treatment may not be justified because the angular dependence of the magnetic waves in the fluid core cannot be correctly represented by a single spherical harmonics. For example, the analysis by Reese, Fincon, & Rieutord (2004) of toroidal modes in a fluid shell have employed finite series expansions of long length for the perturbations.

In this paper, using the method of series expansions of perturbations we calculate toroidal modes of a strongly magnetized neutron star having a fluid core and a solid crust, where the entire interior is assumed to be threaded by a poloidal magnetic field. We employ two different sets of oscillation equations, one for fluid regions and the other for the solid crust, and solutions in the solid and fluid regions are matched at the interfaces between them to obtain an entire solution of a mode. The method of calculation we employ is presented in §2, and the numerical results are given in §3, and conclusions are in §4.

2 METHOD OF SOLUTION

2.1 Magnetic Fields in the Interior

We employ an inner magnetic field of Ferraro (1954) type. For a magnetized star in hydrostatic equilibrium, Ferraro (1954) assumed an interior poloidal field given by

$$B_r = \frac{1}{r^2 \sin \theta} \frac{\partial}{\partial \theta} U, \quad B_\theta = -\frac{1}{r \sin \theta} \frac{\partial}{\partial r} U, \quad (1)$$

where U is a scalar function, and looked for a particular solution to the partial differential equation:

$$\frac{1}{r \sin \theta} \left[\frac{\partial^2 U}{\partial r^2} + \frac{\sin \theta}{r^2} \frac{\partial}{\partial \theta} \left(\frac{1}{\sin \theta} \frac{\partial}{\partial \theta} U \right) \right] = \kappa r^2 \sin^2 \theta, \quad (2)$$

where κ is a constant to be determined. Assuming the scalar function U is given by

$$U = (C_1 r^2 + C_2 r^4) \sin^2 \theta, \quad (3)$$

and imposing the condition that the interior field is continuous at the stellar surface with the outside dipole field, Ferraro (1954) obtained

$$C_1 = -\frac{5}{4} B_p, \quad C_2 = \frac{\kappa}{10} = \frac{3}{4} \frac{B_p}{R^2}, \quad (4)$$

where B_p denotes the strength of the magnetic dipole field at the pole, and R is the radius of the star. For modal analysis shown below, we use this equilibrium magnetic field configuration with B_p being a parameter.

2.2 Oscillation Equations

We assume the temporal and azimuthal angular dependence of perturbations is given by a single factor $e^{i(m\phi + \omega t)}$ for oscillations of magnetized, non-rotating stars, where ω is the oscillation frequency in the inertial frame, and m denotes the azimuthal wave number. The linearized basic equations governing axisymmetric ($m = 0$) toroidal modes propagating in the solid crust of the magnetized star may be given by

$$-\omega^2 \xi_\phi = \frac{1}{\rho} [\nabla \cdot \boldsymbol{\sigma}']_\phi + \frac{1}{4\pi\rho} [(\nabla \times \mathbf{B}') \times \mathbf{B}]_\phi, \quad (5)$$

$$\mathbf{B}'_\phi = [\nabla \times (\boldsymbol{\xi} \times \mathbf{B})]_\phi. \quad (6)$$

In equation (5), $\boldsymbol{\sigma}'$ denotes the Euler perturbation of the stress tensor and is obtained from the Lagrangian perturbation defined in Cartesian coordinates by

$$\delta\sigma_{ij} = (\Gamma_1 p u) \delta_{ij} + 2\mu(u_{ij} - \frac{1}{3} u \delta_{ij}) \quad (7)$$

with u_{ij} being the strain tensor defined by

$$u_{ij} = \frac{1}{2} \left(\frac{\partial \xi_i}{\partial x_j} + \frac{\partial \xi_j}{\partial x_i} \right), \quad (8)$$

where δ_{ij} denotes the Kronecker delta, μ is the shear modulus, and $u = \sum_{l=1}^3 u_{ll}$ (see, e.g., McDermott et al 1988, and Lee & Strohmayer 1996). The linearized equations for toroidal modes in the fluid regions are obtained by simply dropping the term $\rho^{-1} \nabla \cdot \boldsymbol{\sigma}'$ in equation (5).

Since separation of variables is not possible for oscillations of magnetized stars, we employ series expansions of a finite length j_{\max} for the displacement vector $\boldsymbol{\xi}$ and the perturbed magnetic field \mathbf{B}' using spherical harmonic functions $Y_l^m(\theta, \phi)$ for a given m . We have for axisymmetric toroidal modes

$$\frac{\xi_\phi}{r} = - \sum_{j=1}^{j_{\max}} T_{l'_j}(r) \frac{\partial}{\partial \theta} Y_{l'_j}^m(\theta, \phi) e^{i\omega t}, \quad (9)$$

$$\frac{B'_\phi}{B_0} = - \sum_{j=1}^{j_{\max}} b_{l'_j}^T(r) \frac{\partial}{\partial \theta} Y_{l'_j}^m(\theta, \phi) e^{i\omega t}, \quad (10)$$

where $l_j = |m| + 2(j-1)$ and $l'_j = l_j + 1$ for even modes, and $l_j = |m| + 2j - 1$ and $l'_j = l_j - 1$ for odd modes, respectively, and $j = 1, 2, 3, \dots, j_{\max}$, and B_0 is a normalizing constant, which is set equal to B_p . Note that, for axisymmetric toroidal modes with $m = 0$, we have to redefine l_j and l'_j as $l_j = 2j$ and $l'_j = l_j - 1$ for even modes, $l_j = 2j - 1$ and $l'_j = l_j + 1$ for odd modes for $j = 1, 2, 3, \dots, j_{\max}$. Most of the numerical results shown below are obtained for $j_{\max} = 20$. In this convention, the angular pattern of B'_ϕ (of ξ_ϕ) at the stellar surface is symmetric (anti-symmetric) about the equator for even modes and it is anti-symmetric (symmetric) for odd modes.

If we use as dependent variables the vectors \mathbf{t} and \mathbf{b}^T defined by

$$\mathbf{t} = (T_{l'_j}(r)), \quad \mathbf{b}^T = (b_{l'_j}^T(r)), \quad (11)$$

the oscillation equations for fluid regions are given by

$$\frac{B_1}{B_0} \mathbf{Q}_1 \hat{C}_0 r \frac{d}{dr} \mathbf{it} = \hat{C}_1 i \mathbf{b}^T - \left[\frac{B_1}{B_0} \left(2 + \frac{d \ln B_r}{d \ln r} \right) \mathbf{Q}_1 - \frac{B_2}{B_0} \mathbf{C}_1 \right] \hat{C}_0 \mathbf{it}, \quad (12)$$

$$\frac{B_1}{B_0} \mathbf{Q}_0 \hat{C}_1 r \frac{d}{dr} i \mathbf{b}^T = - \frac{p}{2p_{\text{mag}}} V c_1 \bar{\omega}^2 \hat{C}_0 \mathbf{it} - \left(\frac{B_1}{B_0} \mathbf{Q}_0 - \frac{B_2}{B_0} \mathbf{C}_0 \right) \hat{C}_1 i \mathbf{b}^T, \quad (13)$$

and those for the solid crust are given by

$$\frac{B_1}{B_0} \mathbf{Q}_1 \hat{C}_0 r \frac{d}{dr} \mathbf{it} = \hat{C}_1 i \mathbf{b}^T - \left[\frac{B_1}{B_0} \left(2 + \frac{d \ln B_r}{d \ln r} \right) \mathbf{Q}_1 - \frac{B_2}{B_0} \mathbf{C}_1 \right] \hat{C}_0 \mathbf{it}, \quad (14)$$

$$r \frac{d}{dr} \mathbf{W} = -(3 - V) \mathbf{W} - \left[V c_1 \bar{\omega}^2 \hat{C}_0 + \frac{\mu}{p} (2 \hat{C}_0 + 2 \mathbf{Q}_0 \hat{\mathbf{A}}_1 - \mathbf{\Lambda}_0 \hat{C}_0) \right] \mathbf{it} + \frac{2p_{\text{mag}}}{p} \left[\frac{B_1}{B_0} \left(2 + \frac{d \ln B_r}{d \ln r} \right) \mathbf{Q}_0 + \frac{B_2}{B_0} \mathbf{C}_0 \right] \hat{C}_1 i \mathbf{b}^T, \quad (15)$$

and

$$\mathbf{W} = \frac{\mu}{p} \hat{C}_0 r \frac{d}{dr} \mathbf{it} + \frac{2p_{\text{mag}}}{p} \frac{B_1}{B_0} \mathbf{Q}_0 \hat{C}_1 i \mathbf{b}^T, \quad (16)$$

where $i^2 = -1$, and

$$V = \frac{GM_r \rho}{pr}, \quad c_1 = \frac{(r/R)^3}{M_r/M}, \quad M_r = 4\pi \int_0^r \rho r^2 dr, \quad (17)$$

and G is the gravitational constant, M and R are the gravitational mass and the radius of the star, respectively, and

$$B_1 = B_r / \cos \theta, \quad B_2 = -B_\theta / \sin \theta, \quad (18)$$

and $p_{\text{mag}} = B_0^2 / 8\pi$. The definition of the matrices \mathbf{C}_0 , \mathbf{C}_1 , \mathbf{Q}_0 , \mathbf{Q}_1 , $\mathbf{\Lambda}_0$, and $\mathbf{\Lambda}_1$ is found, for example, in Lee (1993), and the matrices $\hat{\mathbf{C}}_0$, $\hat{\mathbf{C}}_1$, and $\hat{\mathbf{\Lambda}}_1$ are defined by

$$\hat{\mathbf{C}}_0 = \mathbf{C}_0, \quad \hat{\mathbf{C}}_1 = \{\mathbf{C}_1\}, \quad \hat{\mathbf{\Lambda}}_1 = \mathbf{\Lambda}_1 \quad (19)$$

for even modes, and

$$\hat{\mathbf{C}}_0 = \{\mathbf{C}_0\}, \quad \hat{\mathbf{C}}_1 = \mathbf{C}_1, \quad \hat{\mathbf{\Lambda}}_1 = \{\mathbf{\Lambda}_1\} \quad (20)$$

for odd modes, where $\{\mathbf{A}\} = (A_{i,j+1})$ for a matrix $\mathbf{A} = (A_{ij})$.

For the inner boundary condition we require that the functions \mathbf{it} and $i \mathbf{b}^T / r$ are regular at the stellar center. The boundary condition at the stellar surface is given by $i \mathbf{b}^T = 0$. The jump conditions at the solid-fluid interfaces is the continuity of the function \mathbf{it} and of the $r\phi$ component of the traction, the latter of which leads to

$$\left[\frac{\mu}{p} \hat{C}_0 r \frac{d}{dr} i\mathbf{t} + 2 \frac{p_{\text{mag}}}{p} \frac{B_1}{B_0} \mathbf{Q}_0 \hat{C}_1 i\mathbf{b}^T \right]_{\pm} = 0, \quad (21)$$

where $[f(r)]_{\pm} = \lim_{\epsilon \rightarrow 0} [f(r + \epsilon) - f(r - \epsilon)]$.

2.3 Neutron Star Models

We integrate the Tolman-Oppenheimer-Volkoff equation (see, e.g., Shapiro & Teukolsky 1983) to obtain zero temperature ($T = 0$) neutron star models, where no effects of the magnetic field on the equilibrium structure are included. The equation of state used for the inner crust and the fluid core is that given by Douchin & Haensel (2001). The equation of state in the outer crust is that given by Baym, Pethick, & Sutherland (1971), and for the fluid ocean we simply use the equation of state for a mixture of a completely degenerate electron gas and a non-degenerate gas of Fe nuclei. The boundary between the fluid ocean and the outer crust is set rather arbitrarily at the density $\rho = 10^4 \text{ g cm}^{-3}$.

For the solid crust, we employ the average shear modulus μ_{eff} (Strohmyer et al 1991), which in the limit of $\Gamma \equiv (Ze)^2/(ak_B T) \rightarrow \infty$ is given by

$$\mu_{\text{eff}} = 0.1194 \times \frac{(Ze)^2 n}{a}, \quad (22)$$

where n is the number density of the nuclei and a denotes the separation between the nuclei defined by

$$\frac{4\pi}{3} a^3 n = 1, \quad (23)$$

and k_B is the Boltzmann constant.

For modal analyses, we calculate neutron star models of mass $M = 1.245M_{\odot}$ and $M = 0.8967M_{\odot}$. For the former model, the radius and the central pressure and density are $R = 1.18 \times 10^6 \text{ cm}$, $p_c = 10^{35} \text{ dyne/cm}^2$, and $\rho_c = 8.75 \times 10^{14} \text{ g/cm}^3$, respectively. The ratio of the thickness of the crust, Δr_{crust} , to the radius is $\Delta r_{\text{crust}}/R \simeq 0.093$, and the surface ocean above the crust is very thin. For the latter model, the parameters are $R = 1.19 \times 10^6 \text{ cm}$, $p_c = 5 \times 10^{34} \text{ dyne/cm}^2$, $\rho_c = 6.75 \times 10^{14} \text{ g/cm}^3$, and $\Delta r_{\text{crust}}/R \simeq 0.139$, respectively.

Figure 1 plots the frequency ω of the crustal toroidal modes of the two models for low values of harmonic degree l , where $\omega_0 = \sqrt{GM/R^3}$ and $\nu = \omega/2\pi$, and no effects of magnetic field are included. For each value of $l \geq 2$, the lowest frequency mode is the fundamental mode that has no radial nodes of the eigenfunction. There exists no fundamental mode for $l = 1$. The figures show that the fundamental mode frequency rapidly increases with increasing l , but the frequencies of the overtones remain almost constant for varying l . As first discussed by Hansen & Cioffi (1980), the frequency of the fundamental toroidal mode in the solid crust is rather insensitive to the neutron star mass, and that of the overtones is inversely proportional to the thickness Δr_{crust} of the crust, which is consistent with Figure 1.

3 NUMERICAL RESULTS

With our numerical method employed to calculate toroidal modes of a magnetized star, we find numerous solutions to the oscillation equations for a given B_p . Most of the solutions thus obtained, however, are dependent on j_{max} , the length of the expansions, and we have picked up only the solutions that are independent of j_{max} .

In Figure 2 the oscillation frequencies of the toroidal modes of the $M = 1.245M_{\odot}$ model are plotted versus the number of radial nodes of the expansion coefficient iT_{l1} , where the left panel is for $B_p = 5 \times 10^{15} \text{ G}$ and the right panel for $B_p = 10^{16} \text{ G}$, and the filled circles and squares indicate odd and even modes, respectively. The figures clearly show the existence of distinct mode sequences, in each of which the frequency of the mode remains rather constant and increases only slowly as the number of nodes increases.

To compare the two cases of $B_p = 10^{16} \text{ G}$ and $B_p = 5 \times 10^{15} \text{ G}$, we plot in Figure 3 the frequency ratio $\omega(10^{16} \text{ G})/\omega(5 \times 10^{15} \text{ G})$ versus $\omega(5 \times 10^{15} \text{ G})/\omega_0$, where the filled squares and circles are for even and odd modes, respectively. Except for the lowest frequency sequence of the even modes, the ratio is approximately equal to ~ 2 , and it decreases as the radial order increases, indicating that the frequency is approximately proportional to the field strength and is largely determined by the strength of the magnetic field. This is not the case for the lowest frequency sequence, for which the ratio rapidly increases from ~ 1 to ~ 2 as the radial order increases, demonstrating that the response of the oscillation frequency to the field strength is not the same as that for the overtone sequences. We note that the lowest frequency mode found in the figure is a much more slowly increasing function of B_p than the modes in the overtone sequences.

It is convenient to write the mode frequency as

$$\omega_p(k, n) = \omega_b + (k + j_p)\Delta\omega + (n - k)\delta\omega + \delta(k, n), \quad (24)$$

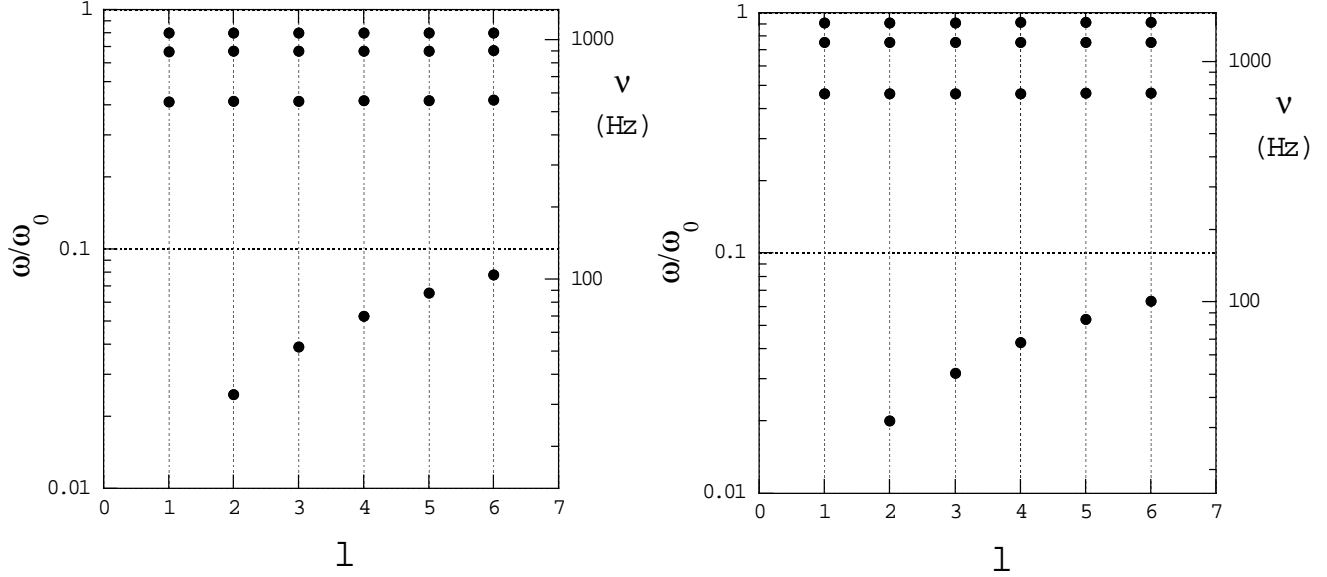


Figure 1. Frequencies of the crustal toroidal modes for low degree ls , where $\omega_0 = \sqrt{GM/R^3}$ and $\nu = \omega/2\pi$, and no effects of magnetic fields are included to calculate the modes. The left panel is for the $M = 0.8967M_\odot$ model, and the right panel for the $M = 1.245M_\odot$ model, respectively. For each value of $l \geq 2$, the lowest frequency mode is the fundamental mode having no radial nodes of the eigenfunction. No fundamental mode exists for $l = 1$.

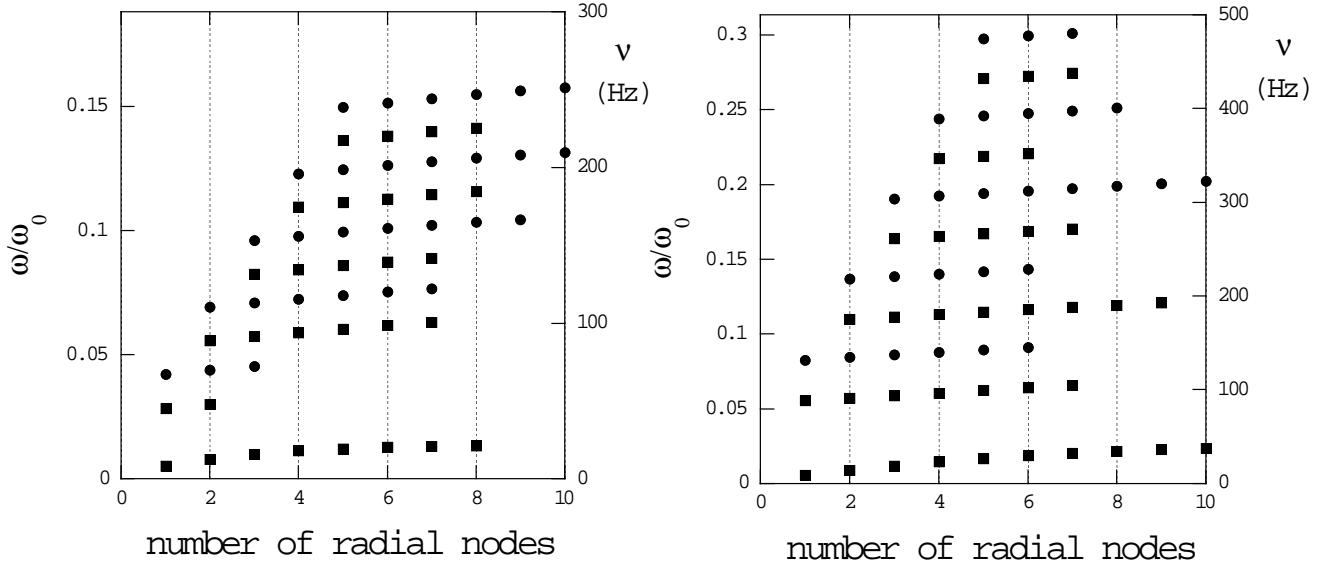


Figure 2. Frequencies of toroidal modes of the $M = 1.245M_\odot$ model versus the number of radial nodes of iT_{l1} , where $\omega_0 = \sqrt{GM/R^3}$ and $\nu = \omega/2\pi$, and the filled squares and circles denote even and odd modes, respectively. The left panel is for the case of $B_p = 5 \times 10^{15} \text{G}$, and the right panel for $B_p = 10^{16} \text{G}$. No fundamental modes without radial nodes are found.

where the non-negative integer k denotes the order of the mode sequences of a given parity (even or odd), and the integer $n(\geq k)$ is the number of nodes of the expansion coefficient iT_l , and the integer j_p is set equal to 0 for the even mode sequences ($p = e$) and to 1/2 for the odd mode sequences ($p = o$). Since there exists no fundamental modes that have no radial nodes of the expansion coefficients, we require $n \geq 1$ even for $k = 0$, for which we have to replace n with $n - 1$ in equation (24). The quantities ω_b , which is set equal to the lowest frequency obtained, $\Delta\omega$, and $\delta\omega$ are assumed independent of k and n , and the quantity $\delta(k, n)$ is assumed to be substantially small compared with $\Delta\omega$ and $\delta\omega$. Note also that we find no mode sequence having $k = 0$ for odd modes, and hence we have to start with $k = 1$ for them. Except for the case that involves the lowest frequency sequence of even modes, $\omega_p(k + 1, n) - \omega_p(k, n) = \Delta\omega + \delta(k + 1, n) - \delta(k, n)$ does not strongly depend on k and n , and $\omega_p(k, n + 1) - \omega_p(k, n) = \delta\omega + \delta(k, n + 1) - \delta(k, n)$ slowly decreases as n increases. It is interesting to note that the quantity $\Delta\omega$ is approximately proportional to the field strength B_p , but the quantity $\omega_p(k, n + 1) - \omega_p(k, n)$ is rather

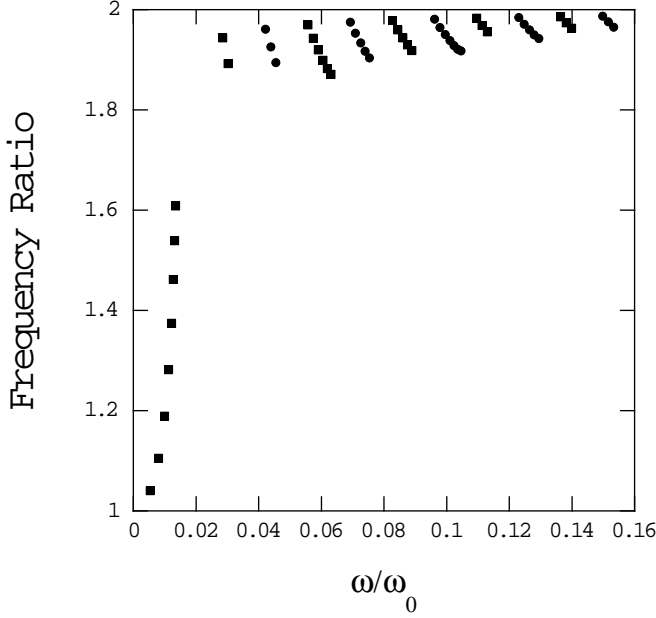


Figure 3. Frequency ratio $\omega(10^{16}\text{G})/\omega(5 \times 10^{15}\text{G})$ versus $\omega(5 \times 10^{15}\text{G})/\omega_0$ for the model of $M = 1.245M_\odot$, where the filled squares and circles are for even and odd modes, respectively.

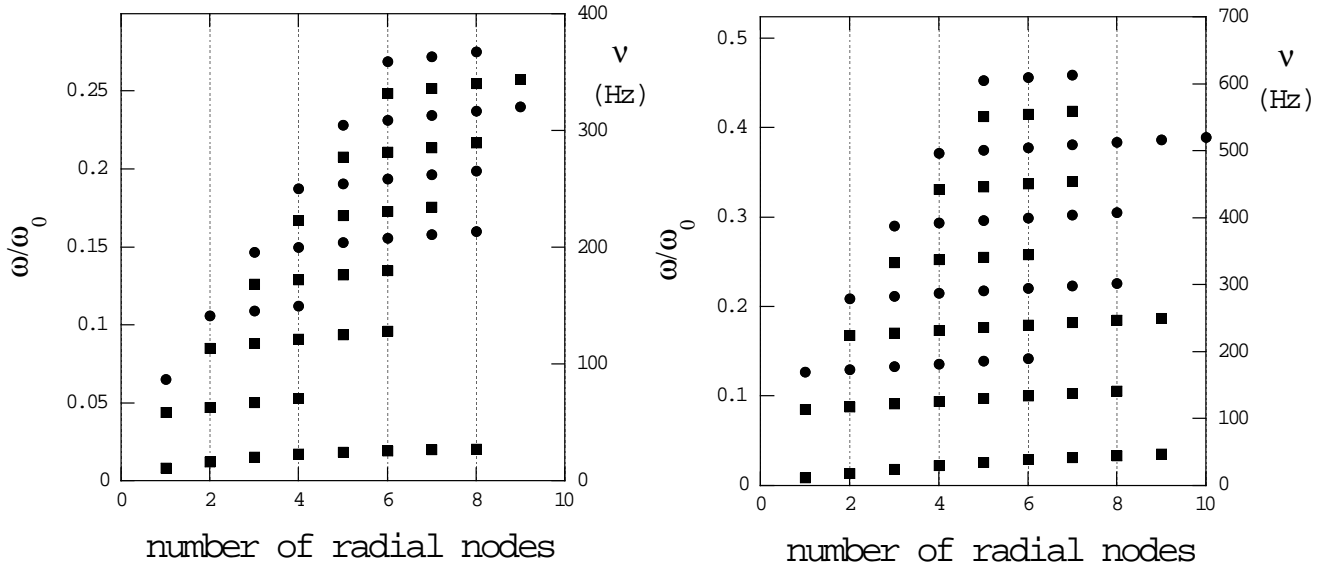


Figure 4. Same as Figure 2 but for $M = 0.8967M_\odot$.

insensitive to B_p . For example, for the model of $M = 1.245M_\odot$, we have $\Delta\omega/\omega_0 \simeq 0.052$ for $B_p = 10^{16}\text{G}$ and $\Delta\omega/\omega_0 \simeq 0.0255$ for $B_p = 5 \times 10^{15}\text{G}$, and $\delta\omega/\omega_0 \simeq 0.0017$ for both cases.

Figure 4 is the same as Figure 2 but for the model of $M = 0.8967M_\odot$, the crust of which is thicker than that of the $M = 1.245M_\odot$ model. Although the frequency spectra look almost the same between the two models, for a given set of (p, k, n) and B_p , the frequency found for the $M = 0.8967M_\odot$ model is higher than that for the $M = 1.245M_\odot$ model. This is because the fluid core radius $R - \Delta r_{\text{crust}}$ (the Alfvén velocity $v_A \propto B_p/\sqrt{\rho}$) of the $M = 0.8967M_\odot$ model is smaller (larger) than that of the $M = 1.245M_\odot$ model, and hence the traveling time $(R - \Delta r_{\text{crust}})/v_A$ of magnetic perturbations in the core for the former is shorter than for the latter.

As examples of the eigenfunctions of the toroidal modes, we plot the expansion coefficients $iT_{l'j}$ and $ib_{l'j}^T$ of three even modes as functions of the fractional radius $x = r/R$ in Figures 5 to 7, where the solid, long-dashed, short-dashed, and dotted lines are the expansion coefficients with $j = 1$ to 4, respectively. For the lowest frequency sequence even modes plotted in Figures 5 and 6, the amplitudes $xiT_{l'}$ are much larger than those of $ib_{l'j}^T$, indicating that the kinetic energy is dominating the

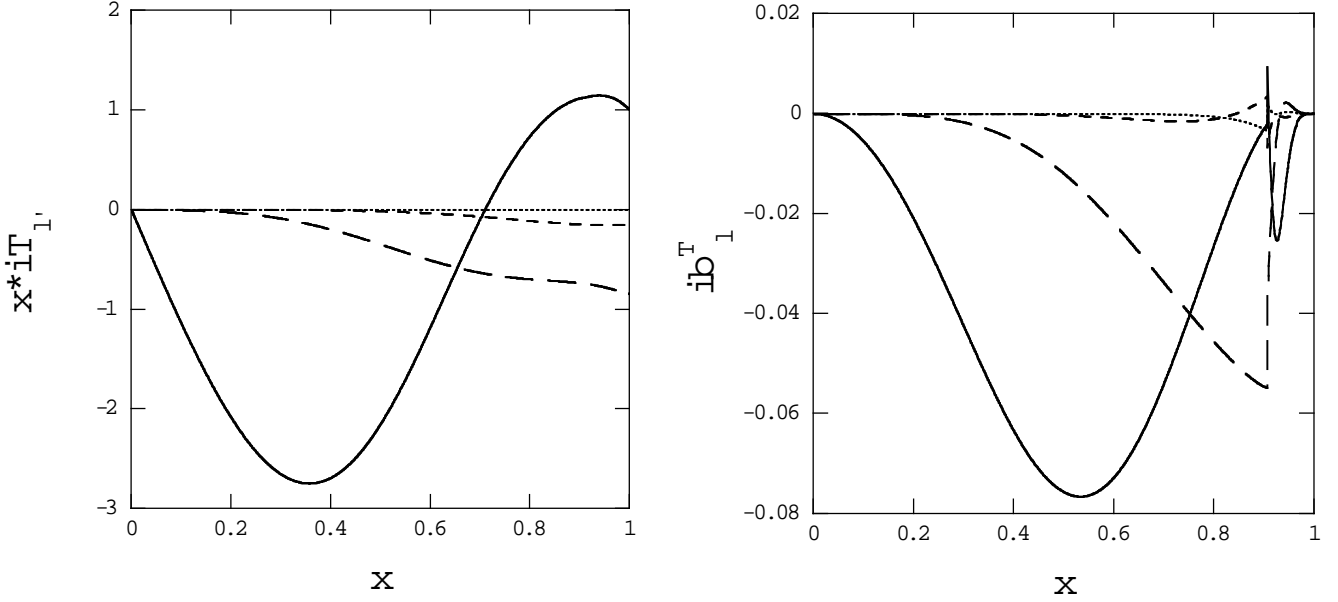


Figure 5. Expansion coefficients $xiT_{l'}$ and $ib_{l'}^T$ as functions of the fractional radius $x = r/R$ for the even toroidal modes of $\omega_e(0, 1)/\omega_0 = 0.005515$ for $B_p = 10^{16}$ G, where $\omega_0 = \sqrt{GM/R^3}$ and $M = 1.245M_\odot$. The solid, long-dashed, short-dashed, and dotted lines are for the expansion coefficients associated with $j = 1$ to 4, respectively. The amplitude normalization is given by $iT_{l'} = 1$ at the stellar surface $x = 1$.

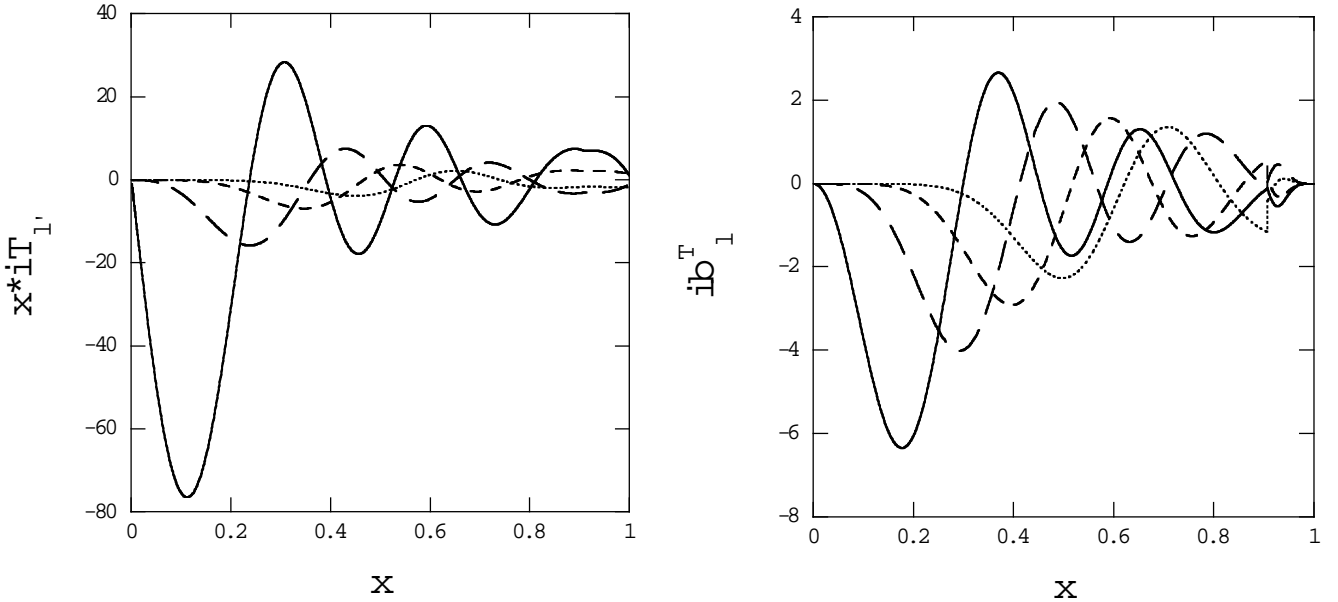


Figure 6. Same as Figure 5, but for the even mode of $\omega_e(0, 5)/\omega_0 = 0.01671$.

magnetic energy. The magnetic perturbations ib_l^T have amplitudes also in the solid crust. This is not the case for the modes in the overtone mode sequences having $k \geq 1$ as exemplified by Figure 7, where the amplitudes of the magnetic perturbations are much larger than $xiT_{l'}$ and are strongly confined in the fluid core, having almost no amplitudes in the crust. Also note that the expansion coefficients with different values of j seem to coalesce to a single curve in the outer core of the star.

Figures 8 to 10 give plots of the expansion coefficients $iT_{l'}$ and ib_l^T for three odd toroidal modes associated with $(k, n) = (1, 1)$, $(1, 5)$, and $(5, 5)$. The magnetic perturbations ib_l^T of the modes have much larger amplitudes than $xiT_{l'}$ and they are strongly confined in the fluid core. The functions $xiT_{l'}$ have comparable amplitudes both in the fluid core and in the solid crust. As in the case of even modes, the expansion coefficients of the mode $(5, 5)$ tend to coalesce to a single curve in the outer core region.

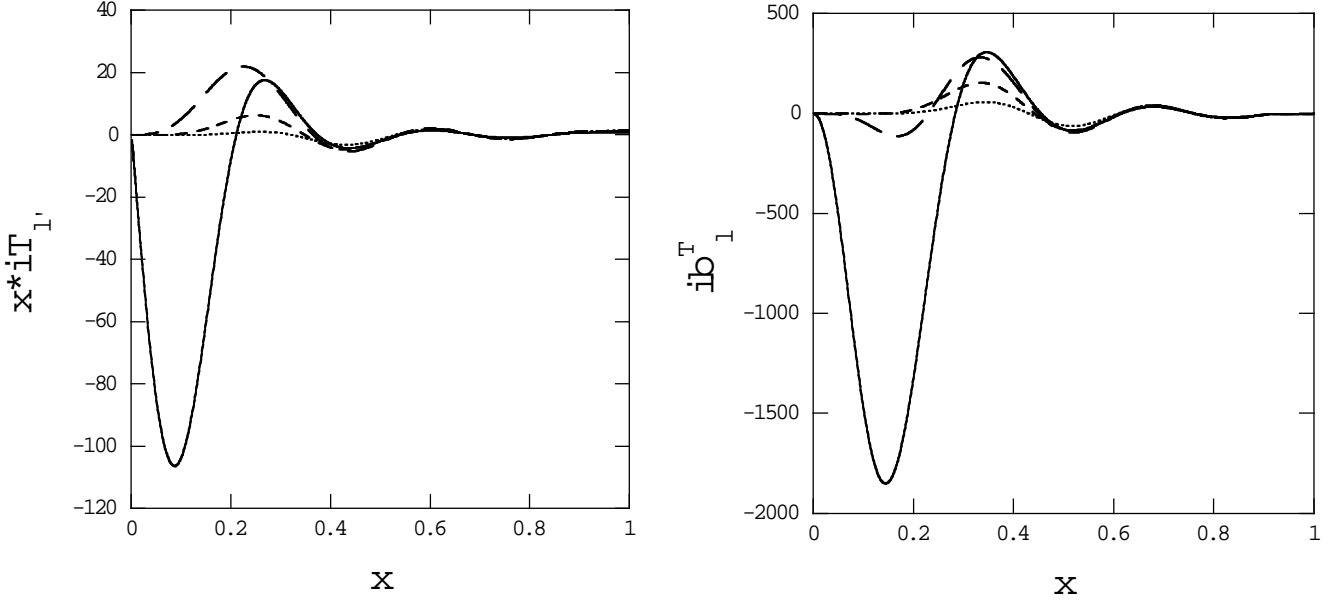


Figure 7. Same as Figure 5, but for the even mode of $\omega_e(5, 5)/\omega_0 = 0.2709$.

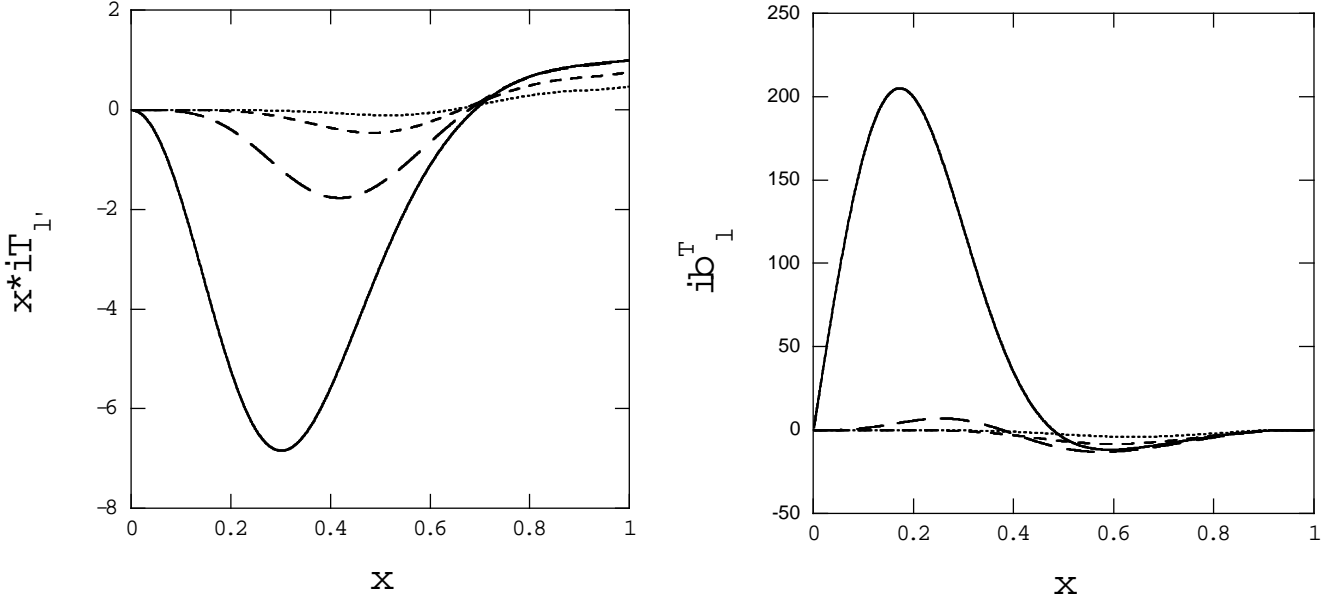


Figure 8. Expansion coefficients $x i T_{l_j}'$ and $i b_{l_j}^T$ as functions of the fractional radius $x = r/R$ for the odd toroidal modes of $\omega_o(1, 1)/\omega_0 = 0.08271$ for $B_p = 10^{16} \text{G}$, where $\omega_0 = \sqrt{GM/R^3}$ and $M = 1.245 M_\odot$. The solid, long-dashed, short-dashed, and dotted lines are for the expansion coefficients associated with $j = 1$ to 4, respectively. The amplitude normalization is given by $i T_{l_1}' = 1$ at the stellar surface $x = 1$.

We need to examine how the existence of a solid crust affects the frequency spectrum of the toroidal modes. Figure 11 shows the toroidal mode frequencies of the $M = 1.245 M_\odot$ model for $B_p = 5 \times 10^{15} \text{G}$, where the modes are calculated by treating the entire interior as a fluid. Without the crust, the lowest frequency sequence is composed of odd modes, and the even mode sequence corresponding to $k = 0$, which appears as the lowest sequence when the solid crust is included, is missing. Therefore, for the fluid star we have to set j_p equal to $j_p = 0$ for odd mode sequences with $p = o$ and to $j_p = 1/2$ for even mode sequences with $p = e$ in equation (24). In the lowest frequency odd mode sequence, there exists the fundamental mode having no radial nodes of the expansion coefficients, corresponding to $(k, n) = (0, 0)$. Since the oscillation equations (12) and (13) for fluid regions contain the oscillation frequency only in the form of the ratio $\bar{\omega}/B_p$, the frequency of a given (p, k, n) is exactly proportional to the field strength B_p . This suggests that the quantities ω_b , $\Delta\omega$, $\delta\omega$, and $\delta(k, n)$ defined in equation

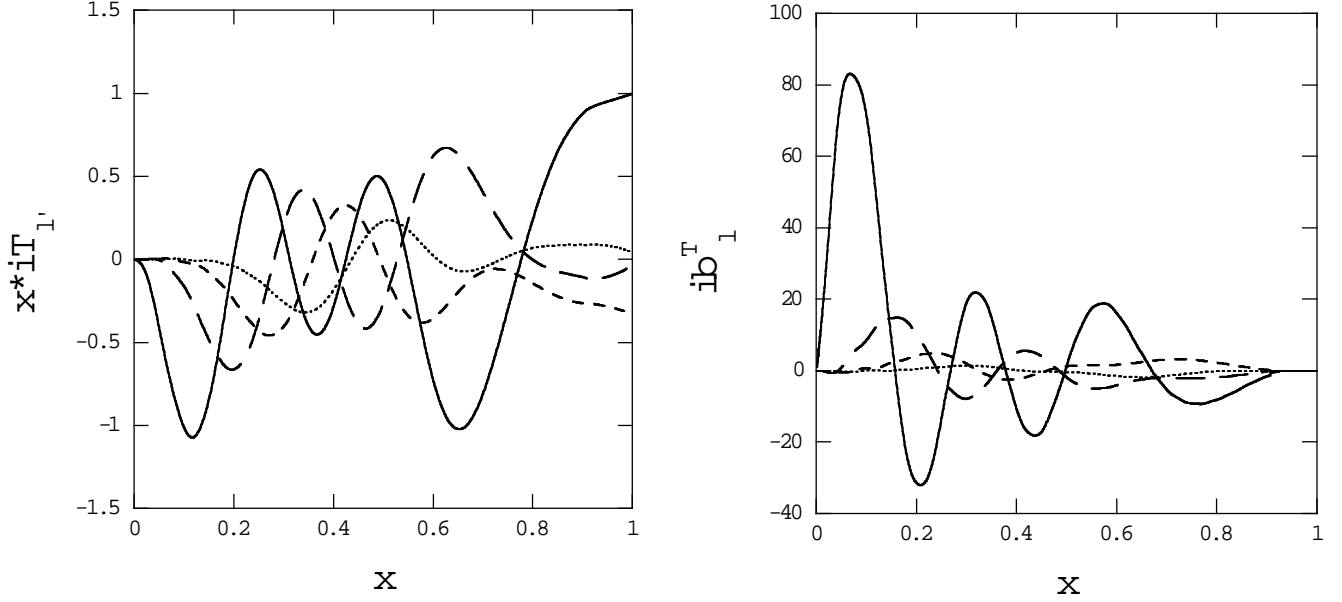


Figure 9. Same as Figure 8, but for the odd mode of $\omega_o(1,5)/\omega_0 = 0.08936$.

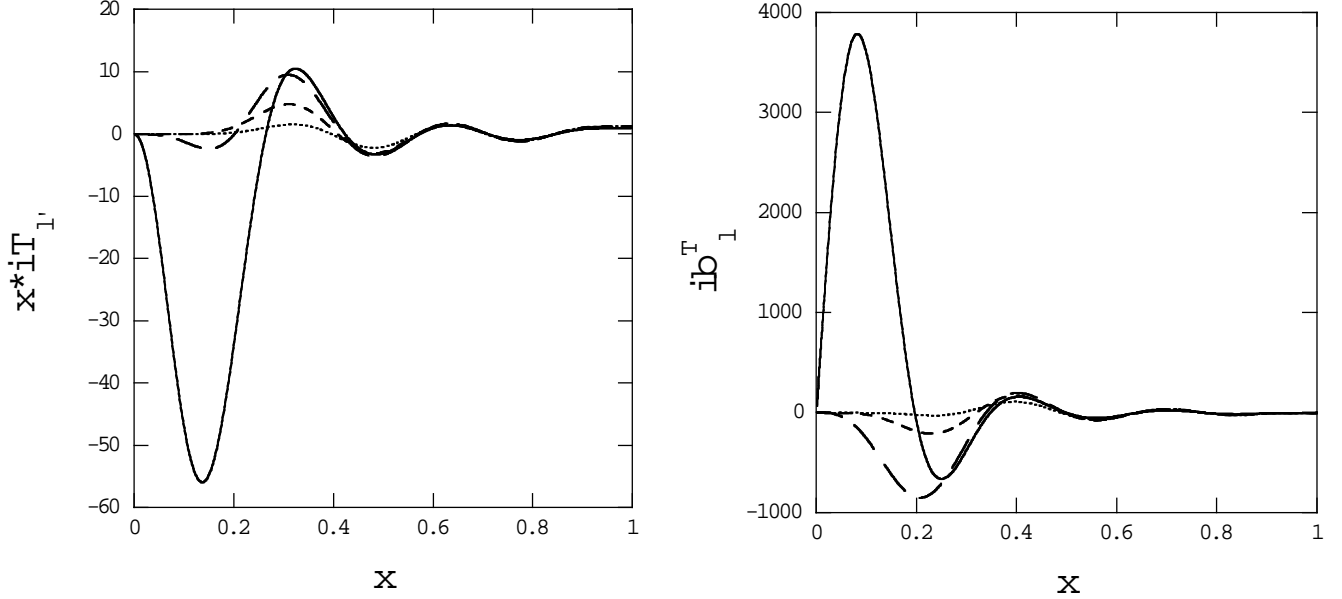


Figure 10. Same as Figure 8, but for the odd mode of $\omega_o(5,5)/\omega_0 = 0.2976$.

(24) are also proportional to B_p . Note that if we write $\omega_b \propto B_p^\beta$ for the lowest frequency mode for the case with a solid crust, where the exponent $\beta > 0$ may be weakly dependent on B_p , we have $\beta \lesssim 1/4$ for $B_p \gtrsim 10^{15}$ G, the feature of which is different from the case without the crust. Figure 11 indicates that the frequency separation between the lowest and second lowest sequences is approximately $\sim \Delta\omega/2$ for the case without the crust, but this separation is given by $\sim \Delta\omega$ for the case with the crust. Note that the frequency separation between the second and third lowest sequences, for example, is given by $\sim \Delta\omega/2$ for both cases.

As suggested by Figures 2, 4, and 11, it is not always possible to numerically find j_{\max} independent modes associated with large values of n and k . Possible numerical reasons for the difficulty may be that the modes we want are immersed in a dense spectrum of j_{\max} dependent solutions, particularly for weak B_p , and that a large j_{\max} and high numerical precision are required to correctly calculate the expansion coefficients in the vicinity of the stellar center for modes associated with large $n \geq k$. From the theoretical point of view, however, it is not necessarily clear that the toroidal modes of the kind we find in this paper exist for arbitrary sets of integers $k(\geq 0)$ and $n(\geq k)$.

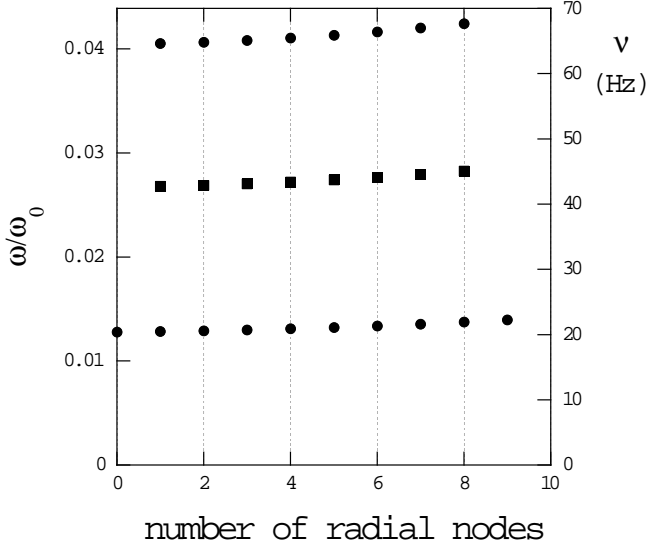


Figure 11. Frequencies of the toroidal modes of the $M = 1.245M_{\odot}$ model versus the number of radial nodes of the expansion coefficient iT_{l1} for $B_p = 5 \times 10^{15}$ G, where $\omega_0 = \sqrt{GM/R^3}$ and $\nu = \omega/2\pi$, and the filled squares and circles are for even modes and odd modes, respectively. The modes are calculated by treating the entire interior as a fluid.

4 CONCLUSIONS

In this paper, we have calculated toroidal modes of magnetized stars with a solid crust, where the entire interior of the star is assumed to be threaded by a poloidal magnetic field that is continuous at the stellar surface to the outside dipole field. We find distinct mode sequences of the toroidal modes, in each of which the mode frequency remains rather constant and only slowly increases as the radial order of the modes increases. In the presence of a solid crust, the frequency separation between the lowest and second lowest frequency mode sequences is approximately given by $\Delta\omega$, but that between the second and third lowest frequency mode sequences by $\Delta\omega/2$, where the frequency separation $\Delta\omega$ is roughly proportional to the field strength B_p . This frequency pattern of the low frequency sequences is different from that found for the model without the crust, for which the frequency separation between the sequential sequences of low frequency modes is given by $\Delta\omega/2$. We also find that for the equation of state we use, $\Delta\omega$ is larger for smaller M .

The eigenfunction ξ_ϕ of the modes belonging to the lowest frequency sequence have much larger amplitudes than B'_ϕ and can penetrate into the solid crust. On the other hand, ξ_ϕ of the modes belonging to the higher frequency sequences is much smaller than B'_ϕ , which is well confined into the fluid core and does not have any substantial amplitudes in the solid crust.

The frequency ranges of the toroidal modes we find for the magnetized neutron star with $B_p \sim 10^{16}$ G overlap the QPO frequencies found for the magnetar candidates, SGR 1806-20 and SGR 1900+14. This suggests that we may interpret the observed QPOs based on the magnetic toroidal modes, and that detailed comparisons between observed frequency spectra and theoretical calculations make it relevant to infer physical parameters of the magnetar candidates, such as the equation of state and the strength of the magnetic field. But, we think it worth pointing out that except for the modes belonging to the lowest frequency sequence, the magnetic perturbations, which have much larger amplitude than ξ_ϕ , are well confined in the fluid core and do not have substantial amplitudes in the solid crust, which make it difficult for the modes to be directly observable. If the magnetar candidates do not have a crust, the problem of observability could be avoided. In this case, however, we have to use more realistic surface boundary conditions than $\mathbf{B}' = 0$ used in the present calculations. Note that, although the existence of a solid crust affects the frequency pattern of the low frequency mode sequences, the frequency range of the magnetic modes itself is not very much dependent on the presence or absence of a solid crust unless the crust is extremely thick.

We have tried to find toroidal modes well confined in the solid crust or core toroidal modes that are in resonance with the crustal toroidal modes, but failed. We also find it extremely difficult to identify distinct toroidal mode sequences for magnetic fields weaker than $B_p \lesssim 10^{15}$ G when a solid crust is included in the models. It is therefore not clear whether the toroidal mode sequences of the kind we find in the present paper can survive also for weakly magnetized neutron stars with a solid crust. If the field strength is much weaker than $B_p \sim 10^{15}$ G, the magnetic fields may have only minor effects on the crustal toroidal modes (e.g., Lee 2007), and it will be justified to use frequency spectra of the crust modes theoretically obtained in the weak field limit to interpret observed QPOs. As briefly noted in the last section, it is not theoretically clear how the frequency spectra of the toroidal modes of magnetized stars should look like, and how the toroidal modes behave in the limit of $n \geq k \rightarrow \infty$. We may even speculate that the frequency spectra we obtained reflect the existence of continuous spectra (see,

e.g., Goedbloed & Poedts 2004, see also Levin 2007), but the detailed numerical analysis of continuous frequency spectra is beyond the scope of this paper. It will be worthwhile to examine the effects of an interior toroidal field on magnetic modes. It is also needed to extend the present analysis to a general relativistic formulation (e.g., Sotani et al 2006, 2007).

REFERENCES

- Baym G., Bethe H.A., Pethick C., 1971, Nucl. Phys., A175, 225
Douchin F., & Haensel P., 2001, A&A, 380, 151
Duncan R.C., 1998, ApJ, 498, L45
Ferraro V.C.A., 1954, ApJ, 119, 407
Goedbloed H., Poedts S., 2004, Principles of Magnetohydrodynamics with Applications to Laboratory and Astrophysics (Cambridge University Press, Cambridge)
Glampedakis K., Samuelsson L., Andersson N., 2006, MNRAS, 371, L74
Hansen C.J., Cioffi D.F., 1980, ApJ, 238, 740
Israel G., et al., 2005, ApJ, 628, L53
Lee U., 1993, ApJ, 405, 359
Lee U., 2007, MNRAS, 374, 1015
Lee U., Strohmayer T.E., 1996, A&A, 311, 155
Levin Y. 2007, MNRAS, 377, 159
McDermott P.N., Van Horn H.M., Hansen C.J., 1988, ApJ, 325, 725
Piro A.L., 2005, ApJ, 634, L153
Reese D., Rincon, F., Rieutord M., 2004, A&A, 427, 279
Shapiro S.L., & Teukolsky S.A., 1983, Black Holes, White Dwarfs, and Neutron Stars (John Wiley & Sons, New York)
Sotani H., Kokkotas K.D., Sterioulas N., Vavoulidis M., 2006, astro-ph/0611666
Sotani H., Kokkotas K.D., Sterioulas N., 2007, MNRAS, 375, 261
Strohmayer T.E., Ogata S., Iyetomi H., Ichimaru S., Van Horn H.M., 1991, ApJ, 275, 679
Strohmayer T.E., Watts A.L., 2005, ApJ, 632, L111
Strohmayer T.E., Watts A.L., 2006, ApJ, 653, 593
Watts A.L., Strohmayer T.E., 2006, ApJ, 637, L117
Woods P.M., Thompson, C., 2006, in Compact Stellar X-Ray Sources, ed. W.H.G. Lewin & M. van der Klis (Cambridge: Cambridge Univ. Press)